Supplemental information

Methods:

CD4$^+$ T regulatory cells stain

Peripheral blood mononuclear cells (PBMCs) from healthy donors and STAT5b-deficient patients were purified by Ficoll-Paque Plus density gradient centrifugation (GE Healthcare). A million of PBMCs from healthy donor, a disease control (patient with *FoxP3* mutation), and STAT5b-deficienct patients were stimulated with 10 µg/ml of *Staphylococcus aureus* Enterotoxin B (SEB) by 24 hours. PBMCs were pre-surface stained during 45 min at 4℃. After this time, the cells were recovered, washed and stained for FOXP3 expression. The antibodies were purchased from BD (CD3, UCHT1, CD8, RPA-T8; CD25, M-A251; CD45RO, UCHL1; FOXP3, 259D/C7) and Tonbo biosciences (CD, SK3). The samples were acquired with an LSR-Fortessa (BD) cytometer and analyzed using FlowJo, LLC software version 10.4.2.

VEGF-A expression in murine NK cells

The CD3$^-$NK1.1$^+$ NK cells from *Stat5b*$^{+/+}$ (WT) and *Stat5b*$^{+/-}$ mice were sorted and lysed in peqGOLD TriFast (VWR). The RNA content was isolated and the expression of VEGF-A was analyzed using qPCR. The expression of VEGF-A was normalized to the expression of Ube2d2. Following primers were used: *mVegfa*-for: GCACAGCAGATGTGAATGCAG; *mVegfa*-rev: CGCTCTGAACAAGGCTCACA; *Ube2d2*-for: AGGTCCTGTTGGAGATGATATGTT; *Ube2d2*-rev: TTGGGAAATGAATTGTCAAGAAA.

Statistics

The statistical significance of differences between healthy donors and patients was determined by the Student's *t*-test. Differences between multiple groups were determined by Ordinary one-way ANOVA test. In mouse, the one-way ANOVA and Bonferronis Multiple Comparison Test was applied for statistical analysis of each maturation stage. Statistical analyses were conducted using Prism 7.0 (GraphPad Software).

Clinical details:

In this study, we evaluated two female siblings with STAT5b deficiency. In 2007, the STAT5b deficiency was identified in both siblings who are daughters of consanguineous parents. Sequencing of *Stat5b* gene revealed a homozygous deletion of a single G at the junction of the exon13–intron13 (c.1680delG). Both patients presented with poor post-natal growth, lung disease, elevated GH levels, and abnormally low levels of circulating insulin-like growth factor-I (IGF-I) and IGF-binding protein (IGFBP)-3.[1] In 2013, these patients were referred to Texas Children's Hospital, Houston, TX for treatment.

Patient 1: A 18 years old female with chronic lymphocytic lung disease, severe central obesity, autoimmune hypothyroidism, thoracic compression fracture and short stature due to growth hormone insensitivity. In 2013, she developed rhinovirus and adenovirus infections. She required cidofavir and steroids treatment to clear adenovirus infection. She then developed EBV viremia that required treatment with Rituximab. A year later she was diagnosed with Influenza and type I diabetes (Table 1).

Patient 2: A 17 years old girl with chronic lymphocytic lung disease (lung biopsy showed primarily $CD4^+$ lymphocytic infiltrations with minimal sub-pleural fibrosis), autoimmune hypothyroidism, thoracic compression fracture from prolonged steroids use juvenile idiopathic arthritis (JIA), and short stature due to growth hormone insensitivity (Table 1). Her viral infections included adenovirus, rhinovirus CMV and EBV viremia (required rituximab). Other infections included culture positive for multi-drug resistant *E.*

coli UTI. In 2016, she was diagnosed pulmonary alveolar proteinosis with *Aspergillus terreus* and *Candida albicans* were identified in bronchoalveolar lavage (BAL) sample.

Immunological profiles:

The immunologic profiles from both patients are shown in Table E1. We observed a severe reduction in the total NK cell counts in both patients (Figure 1, A). The patient 1 was characterized with an extreme and progressive reduction of NK cells numbers and percentages. The first immunological studies at presentation to our center showed NK cells in the lower limit of the reference range (Table E1). However, they remained low over time with an abnormal phenotype suggesting the pivotal participation of STAT5b protein in the development, homeostasis, and proliferation of NK cells. B cell populations counts were normal to elevated (see Table E1). The patients had a long history of pulmonary infections since infancy and poor specific antibody responses (historical clinical data and personal communication) for which they have been on prolonged immunoglobulin replacement. These patients had moderate CD4 and CD8 T cell lymphopenia. We observed higher number of $CD4^+CD45RO^+$ with a skewed CD45RA/CD45RO ratio suggesting a chronic activated dysregulated T cell phenotype [2] (Table E1). Depending on the inflammatory state of the patients at the time the lymphocyte counts were taken, there can be variability in the T and B cell levels. This variability has been previously described. [2]

STAT5b is required for transcription of *FOXP3, CD25, and Bcl-2* [3, 4] The $CD4^+CD25^+$ cell subset, referred to as T regulatory cells (Treg), is characterized by higher expression of FOXP3; however, our results showed an absence of

$CD4^+CD25^+FOXP3^+$ cells in STAT5b-deficient patients and in a disease control (IPEX-patient) compared to healthy control (see Fig E7, A). Moreover, after Staphylococcal Enterotoxin B (SEB) stimulation, both patients had severe reduction of $CD4^+CD25^+FOXP3^+$ cell counts representing only 2.39% (Pt 1) and 1.78% (Pt 2) of the total CD4 T cells compared with our healthy control values of 5.61% (see Fig E7, B). Reduced CD25 and FOXP3 expression (referred to as T regulatory cells-Treg cells) observed in our patients, could also be associated with increased susceptibility to opportunistic infections, autoimmunity and an abnormal accumulation and proliferation of lymphocytes.

In vitro, T cell proliferation to mitogens (phytohemagglutinin, concanavalin A, and pokeweed mitogen) was constantly low in both patients compared to our reference values (Table E1). Similar results were observed in response to recall antigens (*Candida*, tetanus toxoid, and *Diphteria antigen*). These results suggest a general functional T cell defect. The low T cell proliferation, higher frequency of $CD4^+CD45RO^+$ cells, and diminution of $CD4^+CD25^+FOXP3^+$ Tregs cells suggests an abnormal mechanism in the peripheral homeostasis.

References

1. Hwa V, Camacho-Hubner C, Little BM, David A, Metherell LA, El-Khatib N, et al. Growth hormone insensitivity and severe short stature in siblings: a novel mutation at the exon 13-intron 13 junction of the STAT5b gene. Horm Res 2007; 68:218-24.
2. Hwa V, Nadeau K, Wit JM, Rosenfeld RG. STAT5b deficiency: lessons from STAT5b gene mutations. Best Pract Res Clin Endocrinol Metab 2011; 25:61-75.
3. Kanai T, Jenks J, Nadeau KC. The STAT5b Pathway Defect and Autoimmunity. Front Immunol 2012; 3:234.
4. Cohen AC, Nadeau KC, Tu W, Hwa V, Dionis K, Bezrodnik L, et al. Cutting edge: Decreased accumulation and regulatory function of CD4+ CD25(high) T cells in human STAT5b deficiency. J Immunol 2006; 177:2770-4.

Table E1

	Pt 1 (#/mm^3)	Pt 2 (#/mm^3)	References values (#/mm^3) >10 – 18 years	Pt 1 (%)	Pt 2 (%)	References values (%) >10 – 18 years
CD3	1446	1207	1014 – 2557	72.7	43.6	54.0 – 78.0
CD4	1016	667	538 – 1569	51.5	24.1	23.3 – 50.3
CD8	366	467	371 – 936	18.4	16.9	14.8 – 34.8
$CD4^+CD45RA^+$	82	54	134 – 969	4.1	2.0	3.3 – 32.9
$CD4^+CD45RO^+$	925	581	301 – 919	46.5	21.0	15.6 – 41.8
$CD19^+$	310	750	204 – 703	15.6	27.1	10.8 – 25.0
$CD19^+CD27^+$	108	73	19 – 131	5.4	2.6	1.0 – 5.2
$CD3^-CD56$, $CD16^+$	158	57	152 – 595	7.9	5	7.0 – 28.0

T cell-proliferation	Pt 1	Pt 2	Reference values		Pt 1		Pt 2		Reference values	
					Net	Index	Net	Index	Net	Index
<u>Mitogens (5 d)</u>				<u>Antigen (5 d)</u>						
Medium	10,300	2,861	215 – 1,161	Medium	14,460		1,079			
PHA (10 μg/mL)	132,231	100,334	163,507 – 415,087	*Candida*	20,259	2.40	3,348	4.10	>2,000 &	>2.0
ConA (50 μg/mL)	127,848	59,932	80,718 – 286,866	*Diphteria*	317	1.02	569	1.53	>2,000 &	>2.0
PWM (100 ηg/mL)	75,809	49,607	37,006 – 157,955	Tetanus tox	561	1.04	2,135	2.98	>2,000 &	>2.0

Serum Ig	Pt 1	Pt 2	References values
IgG, ng/dL	857	959	641 – 1353
IgM, ng/dL	159	89	69 – 295
IgA, ng/dL	47	193	4 – 180
IgE, UI/dL	<1.5	<1.5	1.5 – 43.0

Online Repository material

Figure legends

FIG E1: STAT5a activation is not affected in STAT5b-deficient patients. A, One million of B-lymphocyte cells lines (BLCL) from healthy donors and STAT5b-deficient patients were lysed and immunoblotted for STAT5a, STAT5b, and Actin (loading control). **B**, Nuclear localization of STAT5 in B-cell lines from healthy donors and STAT5b-deficient patients after IL-21 (50 ng/ml) stimulation. Cells were fixed, permeabilized, and stained for phosphorylated STAT5 (red), followed by counterstaining with DAPI (blue). **C**, Graph shows the nuclear colocalization between pSTAT5 and DAPI after IL-21 stimulation. Data shown is a representative set of results from three independent experiments.

FIG E2: NK cell phenotype gating strategy. Cells were first gated for mononuclear cells (SSC-A vs FSC-A) and singles (SSC-H vs SSC-W and FSC-H vs FSC-W). Living cells were gated based on the negative staining for AmCyan and separated in CD45 positive cells. NK cells were identified as $CD56^{bright}CD3^{-}$ and $CD56^{dim}CD3^{-}$ NK cells. Then, all NK cell markers expression was analyzed in total NK cells or in each NK cell subsets.

FIG E3: Immature $CD56^{dim}$ NK cell phenotype in STAT5b-deficient patients. NK cells from healthy donors and STAT5b-deficient patients were analyzed by flow cytometry. **A**, Representative perforin and developmental markers plots in $CD56^{dim}$ NK cell subset from STAT5b-deficient patients and healthy donors. **B**, The percentage of

positive CD56^{dim} NK cells for each receptor of interest was defined using a corresponding fluorescence minus one (FMO). Data from age- and sex-matched healthy donor are included (light blue circles)[30], in addition to data from unmatched controls acquired at the time of the experiment (dark blue circles). Horizontal bars represent means, and the vertical bars indicate standard deviations. Statistical significance was analyzed using the unpaired Student's *t*-test. Data shown are a representative set of results from three independent experiments. ***p*<0.01, ****p*<0.001, *****p*<0.0001. HD, healthy donors (dark blue circle); previously reported healthy female age and gender matched controls (light blue circle); Pt, STAT5b-deficient patients, Pt 1 (red box); Pt 2 (green box).

FIG E4: Lower cytokine production in STAT5b-deficient patients. A, Representative IFN-γ production plots in NK cell subset from STAT5b-deficient patients and a healthy donor. **B**, Percentage of positive CD56^{bright} NK cells for each cytokine of interest was defined using a corresponding fluorescence minus one (FMO). Horizontal bars represent means, and the vertical bars indicate standard deviations. Statistical significance was analyzed using the unpaired Student's *t*-test. Data shown are a representative set of results from three independent experiments. **p*<0.05, ***p*<0.01, ****p*<0.001, *****p*<0.0001. HD, healthy donors (dark blue circle); previously reported healthy female age and gender matched controls (light blue circle);[30] Pt, STAT5b-deficient patients, Pt 1 (red box); Pt 2 (green box). **C**, Functional response of NK cells from healthy donors and patient 1 after IL-12 (10 ng/ml), IL-15 (1 ng/ml), and IL-18 (10 ng/ml) stimulation. **D**, Percentage and counts of NK cells from *Stat5b*$^{+/-}$ compared to WT

mice are shown. **E**, *Vegf-a*- expression was analyzed in NK cells sorted from *Stat5b*$^{+/-}$ compared to WT mice. **F**, Tumor weight relative to body weight from WT and *Stat5b*$^{+/-}$ mice (n=8/genotype).

FIG E5: Decreased expression of activation and adhesion receptors in NK cell subsets from STAT5b-deficient patients. NK cell phenotypes were measured by flow cytometry. The percentage of positive **A**, CD56^{bright} or **B**, CD56^{dim} NK cells for each receptor of interest was defined using a corresponding FMO. Horizontal bars represent means, and the vertical bars indicate standard deviations. Statistical significance was analyzed using the unpaired Student's *t*-test. Results are representative of three independent experiments. *p<0.05, **p<0.01, ***p<0.001. HD, healthy donors (dark blue circle); previously reported healthy female age and gender matched controls (light blue circle);[30] Pt, STAT5b-deficient patients, Pt 1 (red box); Pt 2 (green box).

FIG E6: Lytic granule convergence does not occur through IL-15 signaling. A, Images of fixed cells showing representative NK cells from healthy donor and patient 1 conjugated to susceptible K562 target cells (10:1 ratio) in absence or presence of IL-15 (25 ng/ml). The yellow arrowheads indicate the microtubule-organizing center (MTOC); TL, transmitted light. **B**, Lytic granules convergence, F-actin accumulation, and MTOC polarization in NK cells from healthy donor and patient 1. The statistical differences between healthy donors and patients was determined by Ordinary one-way ANOVA test. *p<0.05. **C**, Specific cytotoxicity assay were performed using the Cr^{51} release protocol. PBMCs from healthy donor or STAT5b-deficient patients were incubated with

K562 target cells in the absence or presence of 25 ng/ml rhIL-15; results from Fig E7, C, are shown as lytic units required to lyse 10% of target cells (LU_{10}). Patients' LU_{10} was normalized to the healthy donor control for each assay.

Figure E7: Decreased $CD4^+CD25^{high}FoxP3^+$ Tregs cells in STAT5b-deficient patients. CD25 and FOXP3 expression were analyzed by flow cytometry for $CD4^+$ T cell from healthy donors, a disease control (IPEX-patient), and STAT5b-deficient patients. **A**, CD25 and FOXP3 expression in $CD4^+$ T cells directly ex vivo and **B**, after their stimulation with SEB by 24 hours.

Fig E1

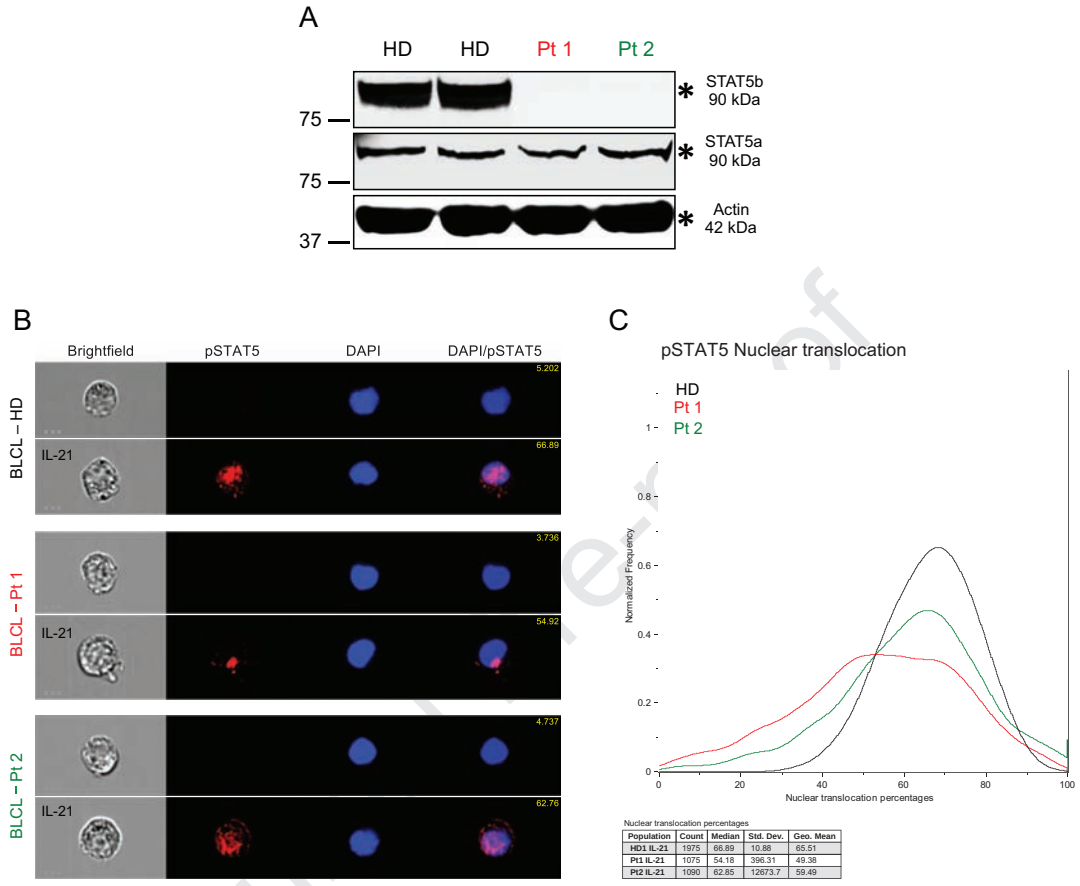
A
HD
HD
Pt 1
Pt 2
75
75
37
STAT5b
90 kDa
STAT5a
90 kDa
Actin
42 kDa
B
Brightfield
pSTAT5
DAPI
DAPI/pSTAT5
BLCL – HD
BLCL – Pt 1
BLCL – Pt 2
IL-21
5.202
66.89
3.736
54.92
4.737
62.76
C
pSTAT5 Nuclear translocation
HD
Pt 1
Pt 2
Normalized Frequency
Nuclear translocation percentages
Nuclear translocation percentages
Population | Count | Median | Std. Dev. | Geo. Mean
HD1 IL-21 | 1975 | 66.89 | 10.88 | 65.51
Pt1 IL-21 | 1075 | 54.18 | 396.31 | 49.38
Pt2 IL-21 | 1090 | 62.85 | 12673.7 | 59.49

Fig E2

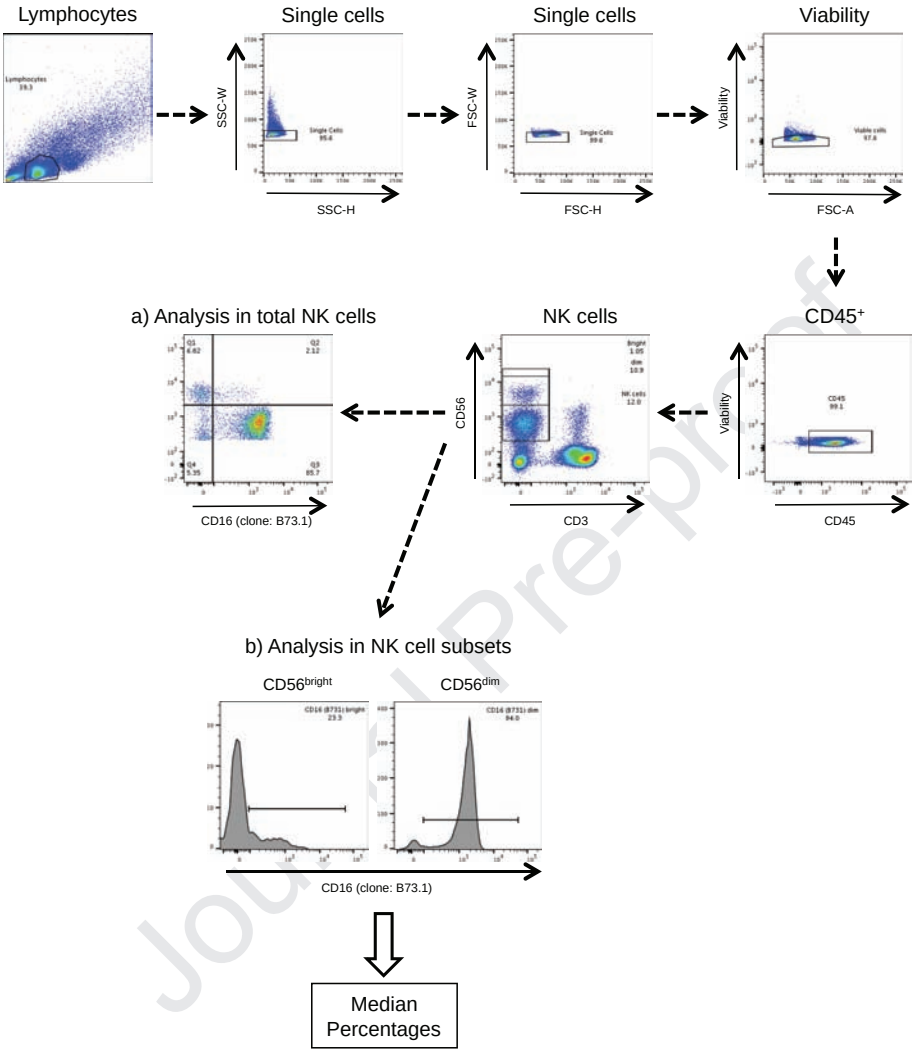

Fig E3

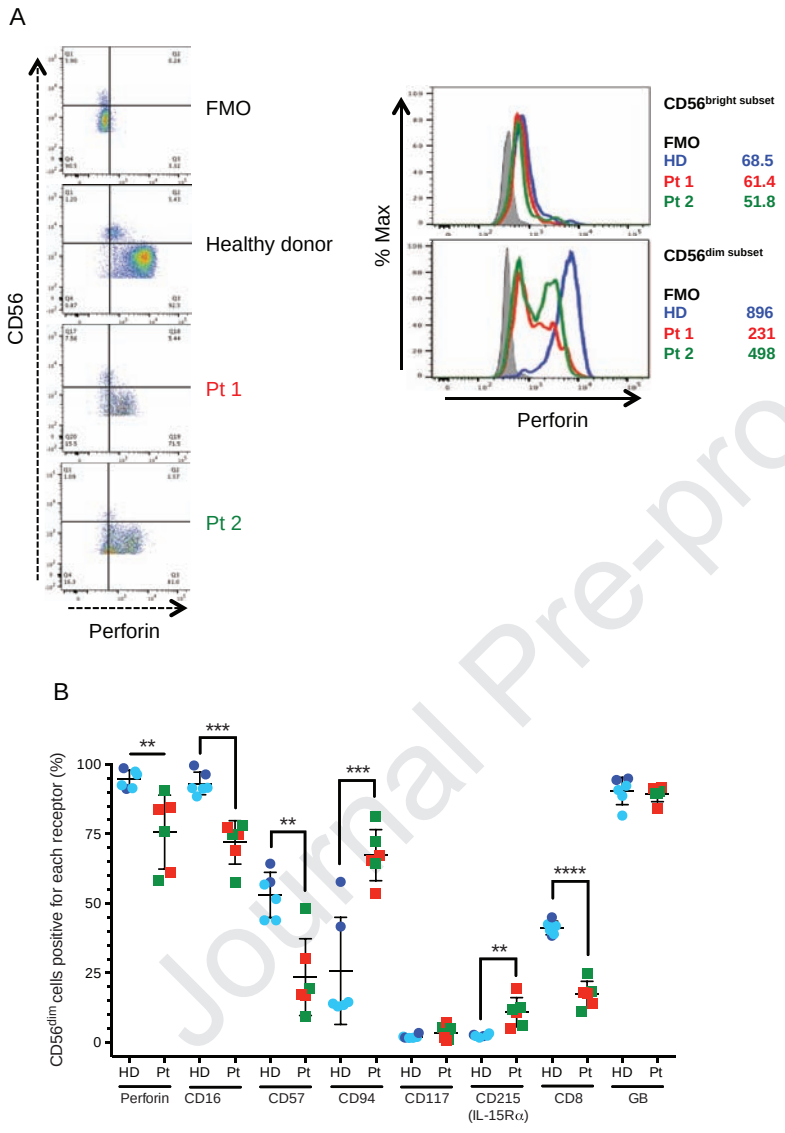

Fig E4

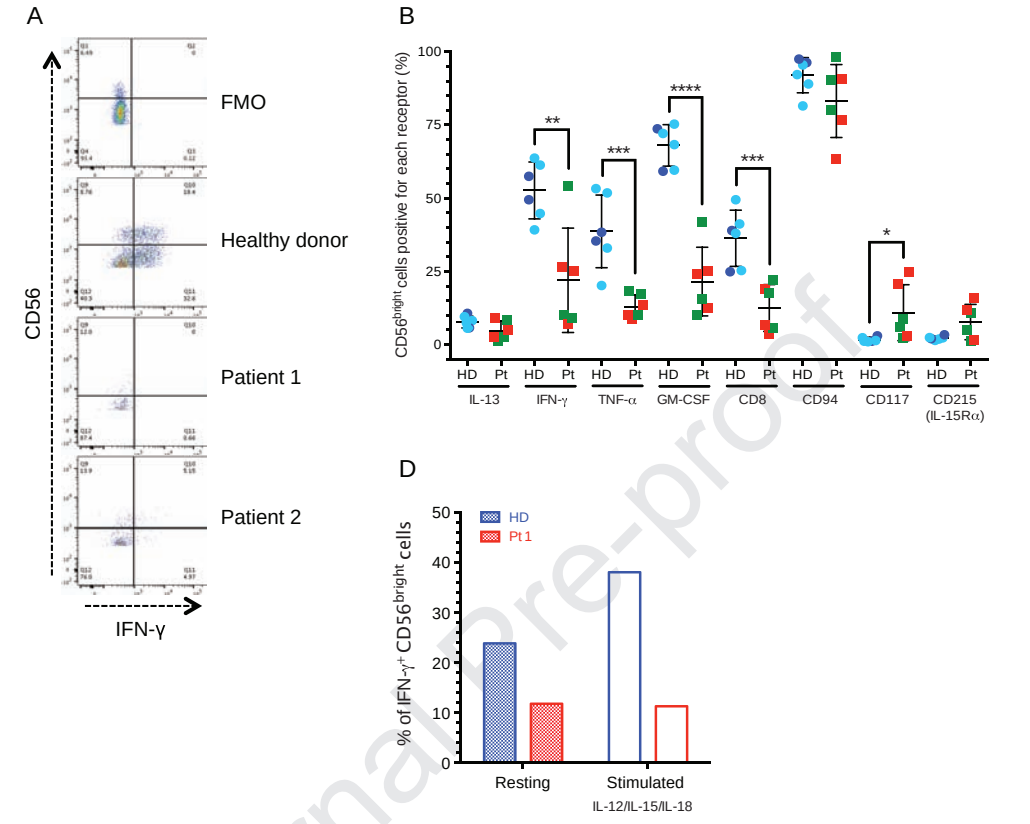

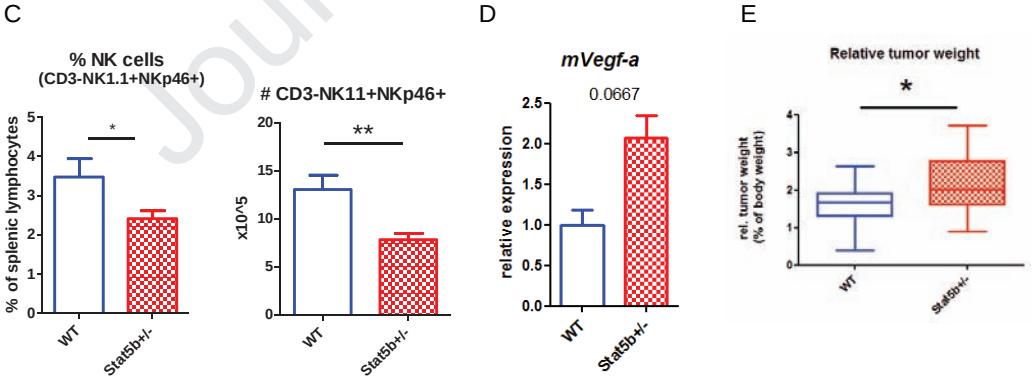

Fig E5

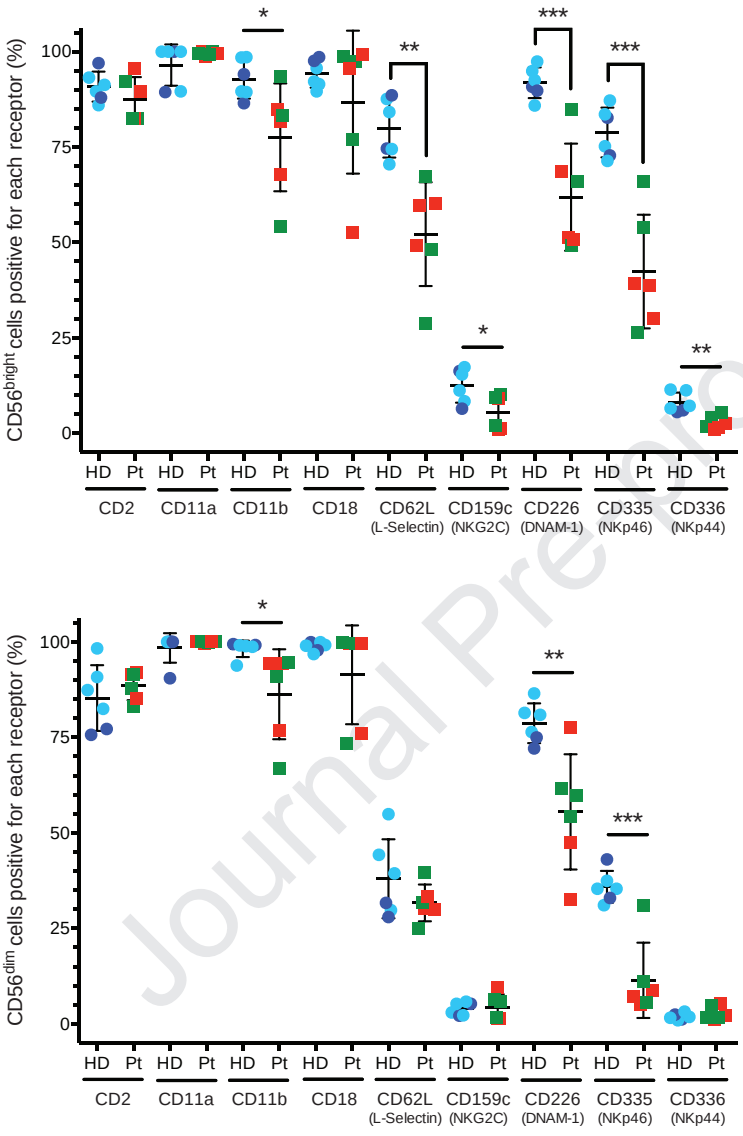

Fig E6

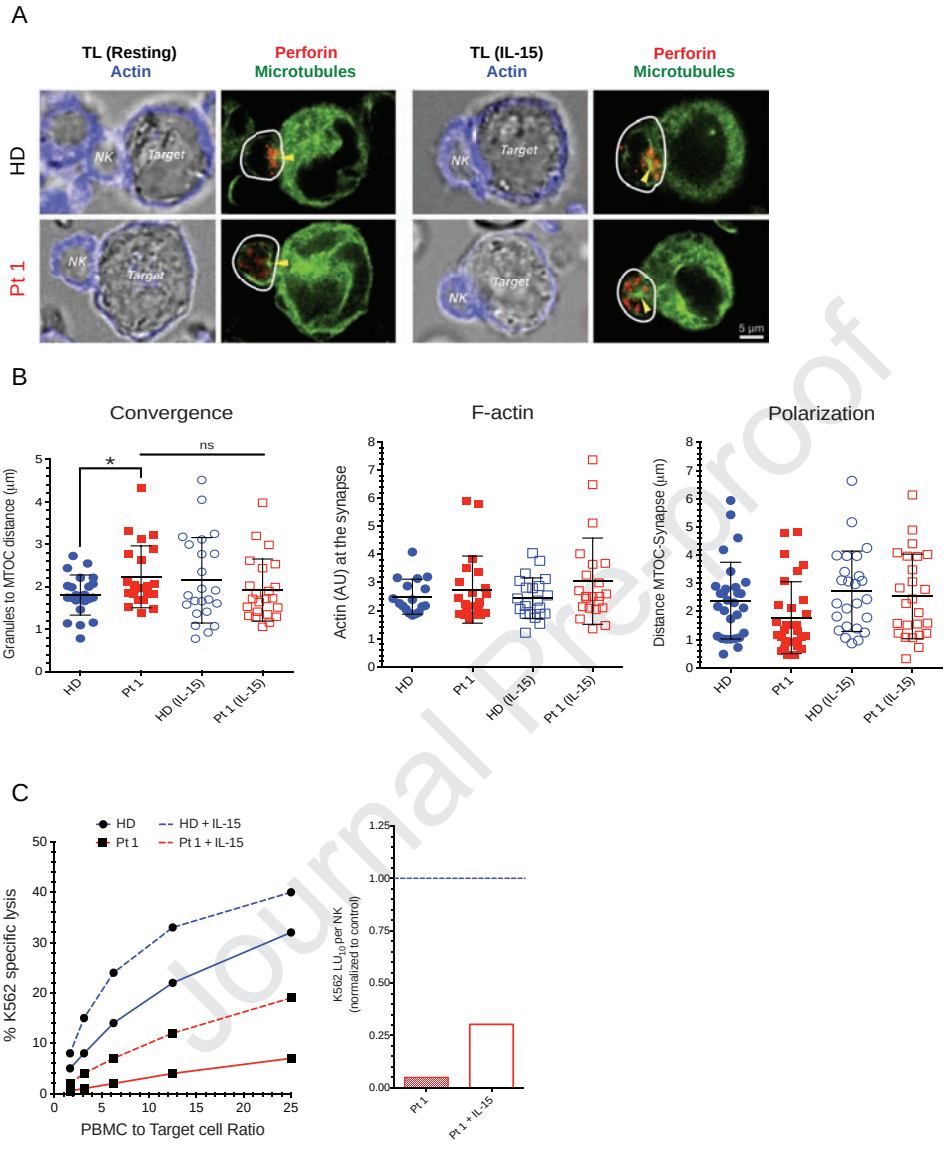

Fig E7

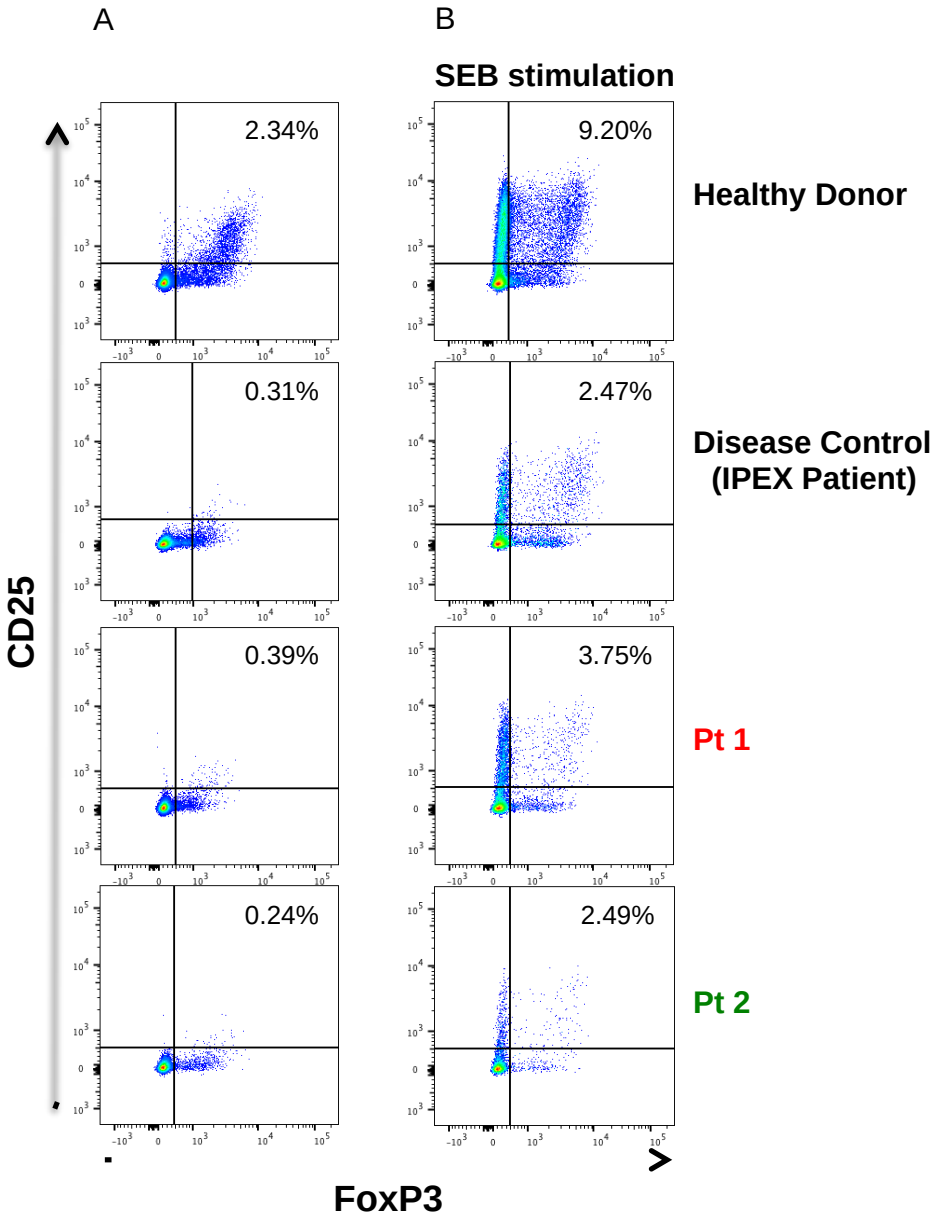
A
B
SEB stimulation
2.34%
9.20%
Healthy Donor
0.31%
2.47%
Disease Control
(IPEX Patient)
0.39%
3.75%
Pt 1
0.24%
2.49%
Pt 2
CD25
FoxP3